



Published in final edited form as:

Am J Transplant. 2015 July ; 15(7): 1768–1781. doi:10.1111/ajt.13189.

Cyclosporine does not prevent microvascular loss in transplantation but can synergize with a neutrophil elastase inhibitor, elafin, to maintain graft perfusion during acute rejection

Xinguo Jiang^{2,3,1}, Tom T. Nguyen^{2,3,1}, Wen Tian^{2,3,1}, Yon K. Sung^{2,3}, Ke Yuan³, Jin Qian^{2,3}, Jayakumar Rajadas⁴, Jean-Michel Sallenave^{6,7}, Nils P. Nickel⁵, Vinicio de Jesus Perez³, Marlene Rabinovitch⁵, and Mark R. Nicolls^{2,3}

²Veterans' Affairs Palo Alto Health Care System, Medical Service, Palo Alto, CA

³Department of Medicine, Division of Pulmonary and Critical Care Medicine, Stanford University School of Medicine, Stanford, CA

⁴Stanford BioADD Laboratory, Stanford, CA

⁵Cardiovascular Institute and Department of Pediatrics, Stanford, CA

⁶Unité de Défense Innée et Inflammation, Institut Pasteur, Paris, France

⁷INSERM U884, Paris, France

Abstract

The loss of a functional microvascular bed in rejecting solid organ transplants is correlated with fibrotic remodeling and chronic rejection; in lung allografts, this pathology is predicted by bronchoalveolar fluid neutrophilia which suggests a role for polymorphonuclear cells in microcirculatory injury. In a mouse orthotopic tracheal transplant model, cyclosporine, which primarily inhibits T cells, failed as a monotherapy for preventing microvessel rejection and graft ischemia. To target neutrophil action that may be contributing to vascular injury, we examined the effect of a neutrophil elastase inhibitor, elafin, on the microvascular health of transplant tissue. We showed that elafin monotherapy prolonged microvascular perfusion and enhanced tissue oxygenation while diminishing the infiltration of neutrophils and macrophages and decreasing tissue deposition of complement C3 and the membrane attack complex, C5b-9. Elafin was also found to promote angiogenesis through activation of the extracellular signal-regulated kinase (ERK) signaling pathway but was insufficient as a single agent to completely prevent tissue ischemia during acute rejection episodes. However, when combined with cyclosporine, elafin effectively preserved airway microvascular perfusion and oxygenation. The therapeutic strategy of targeting neutrophil elastase activity alongside standard immunosuppression during acute rejection

Corresponding author: Mark R. Nicolls, mnicolls@stanford.edu.

¹XJ and TTN and WT contributed equally to this manuscript.

Disclosure:

The authors of this manuscript have no conflicts of interest to disclose as described by the American Journal of Transplantation.

Supporting Information

Additional Supporting Information may be found in the online version of this article.

episodes may be an effective approach for preventing the development of irreversible fibrotic remodeling.

Introduction

Chronic rejection remains the main obstacle to long-term survival in solid organ transplantation. Clinical studies on lung, kidney, liver and heart transplants have shown that microvascular loss precedes the development of chronic rejection (1–5). Consistent with these reports, our group has demonstrated in a mouse orthotopic tracheal transplantation model that a functional microvascular circulation is essential for the health of airway transplants and those grafts lacking a functional microvascular supply inevitably develop fibrosis (6). We further showed that promoting vascular health by enhancing microvascular repair and regeneration during acute rejection leads to better long-term outcomes in airway transplants (7). Collectively, these studies highlighted the notion that a loss of the functional microvasculature may be a root cause of fibrotic remodeling and strategies aimed at enhancing microvascular health may lead to novel therapies for preventing chronic rejection (8).

Neutrophils have long been known to be associated with the injury to transplanted lungs (9). It has also been shown that neutrophil accumulation in airway walls and in the bronchoalveolar lavage (BAL) fluid may increase the risk of developing obliterative bronchiolitis (OB) (10, 11). A recent study showed that hyaluronan-induced OB depends on activation of the innate immunity with subsequent neutrophilia (12). Neutrophil-derived elastases are key modulators of inflammation-induced tissue injury. Destructive elastases, including human neutrophil elastase and proteinase 3, can degrade most components of the extracellular matrix. They are also able to promote tissue inflammation through diverse mechanisms including cleavage of cell surface receptors and liberation of matrix derived fragments (13). Neutrophil elastase is also involved in endothelial cell (EC) injury (14–16). In lung transplant recipients, unopposed neutrophil elastase activity is commonly observed and may be associated with lung injury and the development of OB (17).

Elafin is a low-molecular weight protein that inhibits both neutrophil elastase and proteinase 3; it also plays an anti-inflammatory role by modulating intracellular signaling pathways (18–20). A number of studies have already shown that anti-neutrophil elastase therapies may hold promise for the treatment of diseases associated with lung, bowel and skin inflammation as well as for ischemia-reperfusion injury following myocardial infarction or organ transplantation (13). Additionally, elafin was shown to attenuate coronary arteriopathy in a rabbit heterotopic cardiac transplantation model (21). The effect of elafin in models of lung transplantation has not been studied.

Several animal models have been developed to study the pathophysiology associated with human lung allografts, including heterotopic tracheal, orthotopic tracheal and orthotopic lung transplantation. The orthotopic tracheal transplant model does not model OB but is utilized because the microvessels are configured in a single physical plane; this architecture facilitates the study of the dynamic changes to the entire microcirculatory bed not possible in other models. In this model, the complete transplant microcirculation can be visualized on

a single whole-mount slide. Rejecting tracheas develop lymphocytic bronchitis, a clinically relevant large airway precursor of OB (22). We have used this model to extensively study the phenotypic changes of microvessels in transplanted airways undergoing rejection, and have demonstrated that chronic rejection of the graft can be delayed and/or attenuated by improving the microvascular health of the airway (6, 7, 23–25). Because of the strong association between bronchoalveolar fluid neutrophilia and the development of chronic rejection, we sought to determine the effect of elafin on airway perfusion, oxygenation and tissue remodeling. The main objective of this study was to determine whether simultaneously suppressing neutrophil and T cell activity could lead to better preservation of the airway microvasculature and architecture than that seen with solely targeting adaptive immunity.

Materials and Methods

Mice

All animal procedures were approved by Stanford's Administrative Panel on Laboratory Animal Care (APLAC) and/or the VA Palo Alto Institutional Animal Care and Utilization Committee (IACUC). All mice including C57BL/6J (B6; H-2b) and Balb/C (H-2d) were purchased from Jackson Laboratories.

Tracheal transplantation

Balb/C mice were used as donors. The surgical procedure of tracheal transplantation was carried out as previously described (7). Briefly, donor and recipient mice were matched by age and sex and then anesthetized with 50 mg/kg ketamine and 10 mg/kg xylazine. 5- to 7-ring tracheal segments were removed from donor mice and the donor tracheas were stored in phosphate buffered saline (PBS) on ice before transplantation. AdLacZ was used as control as we described (7). AdElafin and AdSLPI were produced as described (26, 27). For adenovirus gene transfer experiments, donor tracheas were incubated in the adenovirus solution (2×10^{12} vp/ml) for 60 minutes at 4°C before transplantation. A ~2–3 cm incision was made in the midline region of the recipient's neck. The strap muscles were then bluntly divided and pulled aside with 3-0 sutures, which allowed clear exposure of the laryngotracheal complex. After the recipient trachea was transected, donor trachea was sewn in with 10-0 nylon sutures and the skin was closed with 5-0 silk sutures.

Tissue preparation for perfusion studies and histology

For whole-mount tracheal microvascular perfusion analysis, mice were injected with 100 µl of FITC-conjugated tomato lectin (Vector Laboratories) at a concentration of 1 mg/ml through the inferior vena cava. After about 5 minutes of circulation, the mice were perfused with 1% PFA diluted in PBS for about 1 minute. The tracheas were then harvested, put in 1% PFA for 1 hour at 4°C, and then washed 3 times with PBS. Whole tracheas were mounted on glass slides in Vectashield H-1200 mounting medium (Vector Laboratories). Assessment of the percentage of the perfused area was carried out as previously described (23). Briefly, the whole tracheal allograft (every cartilaginous and inter-cartilaginous region) was examined and each area was scored either a 1 if it was perfused or 0 if it was not perfused. The percent perfusion was then calculated as follows: total score/total regions

examined. Paraffin-embedded tracheal segments were initially fixed in cold 10% neutral-buffered formalin solution. 5- μ m sections were cut and stained for H&E and Masson's trichrome staining. Frozen sections were used for other immunohistochemistry analysis. Trachea samples were snap-frozen in OCT solution (Sakura Finetek) after harvest and stored at -80°C . 8- μ m sections were used for immunofluorescence staining. Anti-CD31 (1:200; BD Pharmingen) antibody was used to stain endothelial cells; anti-Ly6G (1:100, Abcam) and anti-myeloperoxidase (1:100, Abcam) were used to stain neutrophils; anti-F4/80 (1:100; eBioscience) and anti-MAC387(1;100; Abcam) were used to stain macrophages; anti-elastase (1:100, Abcam) was used to stain neutrophil elastase; anti-C3d (1:50, R&D) and anti-C5b-9 (1:100, Abcam) were used to study complement deposition; anti-CD4 (1:200) and anti-CD8 (1:200; BD Pharmingen) were used to stain CD4+ and CD8+ T cells respectively. Dihydroethidium (DHE) (20 μ M, Invitrogen) was used to detect reactive oxygen species (ROS) as we described (28). The TUNEL assay (Invitrogen, C10245) to stain for apoptotic cells was carried out according to the manufacturer's protocol. NE680 (PerkinElmer) was used to detect elastase activity as described (29). Photomicrographs were taken with a Zeiss LSM 510 laser scanning confocal microscope coupled with Zeiss LSM Image Browser software.

Western blotting

Protein of cultured endothelial cells was extracted with RIPA buffer that contained both protease and phosphatase inhibitors (Thermo Fisher Scientific). Extracts were incubated on ice for 30 minutes, followed by centrifugation at 18,000 g at 4°C for 15 minutes. Extracts containing 35 μ g of protein were separated on SDS gels and transferred to nitrocellulose membranes. Actin was used as an internal control. Membranes were incubated with anti-p-ERK1/2 (Cell Signaling), anti-ERK1/2 (Cell Signaling), or anti-actin (Sigma-Aldrich) at 4°C overnight. Blots were incubated with the appropriate secondary antibodies and signals were detected by PhosphorImager analysis using ECL Plus (Amersham).

Administration of elafin and cyclosporine (CsA)

Elafin (Proteo Biotech AG) was diluted in PBS and administered at a concentration of 1.9mg/kg/d through a subcutaneous mini-osmotic pump (Alzet, model 2002) from day 0 until sacrifice. CsA stock solution (100mg/ml) was made by dissolving it in ethanol. CsA stock was further diluted in PBS and administered every day from day 0 through intraperitoneal injection.

Tissue oximetry

Tissue oxygen content was measured by the fluorescence quenching technique with the OxyLab pO₂ monitor (Oxford Optronix Ltd.) as previously described (30). To take measurements, the fiber optic probe was placed against the epithelial luminal surface of the trachea.

Blood perfusion monitoring by laser doppler flowmetry

The procedure has been described in detail in (30). In short, the transplanted mice were placed under general anesthesia and the tracheal grafts were carefully exposed by gently

retracting the strap muscles with stay sutures, revealing the anterior wall of the trachea. Perfusion monitoring was performed with a fiber optic laser doppler flowmetry (LDF) probe connected to the OxyLab LDF monitor (Oxford Optronix). The probe was connected to a micromanipulator and gently lowered onto the outer surface of tracheal grafts. This provided a continuous digital readout of blood perfusion units (BPUs) by real-time measurements of red blood cells in flux which is proportional to the red blood cell perfusion. BPU measurements were recorded.

Tube formation assay, scratch assay and migration assay

Tube formation assay—Matrigel (BD Matrigel Basement Membrane Matrix Growth Factor Reduced, Phenol Red Free, 356231) was thawed on ice overnight, dispersed onto 48-well plates (100 μ l per well) and allowed to polymerize for 30 minutes at 37°C. Human umbilical vascular endothelial cells (HUVECs) were seeded on the Matrigel at the density of 1×10^4 cells per well. Images were taken 10 hours later. ImageJ software was used to determine total cellular cord length and branch points.

Migration assay—Cellular migration was evaluated with a modified Boyden chamber assay. Briefly, HUVECs at 3–5 passages were detached from cell culture plates with 0.25 % trypsin and harvested by centrifugation. 2×10^4 HUVECs in 250 μ l of serum free endothelial cell medium (ECM) (Sciencell, Cat#: 1001) were seeded in the upper chamber of transwell cell culture inserts (8 μ m pore size; BD Biosciences). 750 μ l of serum free ECM containing human recombinant vascular endothelial growth factor (VEGF; 1.2 nM, Peprotech), or 0.3 μ M, 0.6 μ M, 1.2 μ M recombinant elafin or 0.6 μ M elafin + 10 μ M PD 98059 (an inhibitor of ERK1/2) were placed in the lower chamber. After incubation for 10h at 37°C, the nonmigrating cells were gently removed from the upper chamber with a cotton swab. The membranes were then washed with PBS and fixed with methanol for 5 mins. Cells were stained with a modified Giemsa solution (Sigma-Aldrich, Cat#: GS500) for quantification. Cells that migrated into the lower chamber were counted manually in five random high-power (100 \times) microscopic fields by independent, blinded investigators and the average number of cells/100 \times field was determined.

Scratch assay— 6×10^5 HUVECs were seeded on an Easy Slide (Millipore) the day before the experiment and allowed to form a fully confluent monolayer. Cells were then starved in serum free medium for 12 hours. A 200 μ l pipet tip was used to scratch a straight line across the middle of the cell monolayer. Cell debris was washed off with PBS. HUVECs were then incubated with serum free medium. Images were taken immediately after scratch and the same windows were imaged again 12 hours later. The rate of cell migration was calculated with ImageJ software as the average percent wound closure from at least 3 independent experiments.

Chemotaxis assay

Neutrophils and macrophages were isolated from peritoneum following 3% thioglycollate treatment for 2 hours and 48 hours, respectively. 2D μ -Slide Chemotaxis chamber (Ibidi, Cat#: 80306) was used for the chemotaxis assay following the manufacturer's instruction.

Freshly isolated neutrophils and macrophages were used for the assay. Images were taken following 6 hours of chemotaxis. ImageJ was then used to analyze the data.

Statistical analysis

Statistical analysis was performed using 1-way ANOVA with Tukey's post test or 2-tailed Student's t-test, with a significance level of $P < 0.05$.

Results

Cyclosporine does not protect airway microvascular perfusion

CsA, a calcineurin inhibitor that blocks T cell activation, is a medication that is routinely used in transplant recipients. While CsA blocks parenchymal rejection in pre-clinical models, including tracheal allografts (31), CsA has not been previously studied with respect to conserving microvascular perfusion specifically. In orthotopic tracheal transplants, the acute rejection phase ranges from d4 to d12 following transplantation. In general, d4 is the time when the free tracheal transplant starts to be perfused, and this perfusion will last until d8; d10 is the time point when the microvasculature loses its perfusion, and d12 marks the late phase of acute rejection in this model (6, 7). Chronic rejection starts on approximately d14 and the airway transplant reaches a stable fibrotic structure on around d28. We have previously demonstrated that protection of a functional microcirculation during acute rejection can delay or even prevent the development of chronic rejection. Therefore, we focused on the acute rejection phase in this study. When CsA was administered at a concentration of 25mg/kg/d, a high dose of CsA previously used in the tracheal study (31), the epithelial layer of the d14 allografts was partially protected. But surprisingly, no microvascular perfusion was observed (Fig. 1A). At this dose, we suspected that CsA could have been injurious to endothelial cells, and that with lower doses, better microvascular perfusion would be observed. Therefore, we examined tissue perfusion using low doses of CsA. Our group has previously shown BPU measured by LDF can be used to serially measure airway perfusion (30). Time course experiments with CsA at doses of 2.5 and 10mg/kg/d revealed that while CsA limited mononuclear cell inflammation, it did not preserve microvascular perfusion (Fig. 1B); tissue ischemia correlates well with BPU readings 150 (23). Thus, at all concentrations tested, CsA did not preserve a functional microvasculature in airway transplants undergoing acute rejection. We questioned whether the inability of CsA to protect the microvascular circulation was because of the toxicity of CsA to endothelial cells or because vascular injury was attributable to non-T cell mediators not targeted by this therapy. We subsequently studied the role of neutrophil elastase in graft ischemia as a possible pathway, not addressed by CsA monotherapy, which could account for the calcineurin inhibitor's failure to protect microvessels.

Increased neutrophil elastase activity in airway transplants undergoing acute rejection

Cells of the innate immune system, such as macrophages and neutrophils, are known to be present in transplants undergoing acute rejection and these cells may induce tissue injury, including endothelial cell death, through various mechanisms such as the production of ROS, IL-1 β and TNF- α (8, 32). Using Ly6G as a marker for neutrophils, we observed a significant infiltration of neutrophils into airways on both 8 and 12 days following

transplantation (Fig. 2A–C). Neutrophil elastase was also abundantly present in d8 transplants (Fig. 2D and E). Correspondingly, d8 allografts displayed elevated neutrophil elastase activity as measured by NE680 staining (Fig. 2F and G). To test whether elevated anti-elastase activity improves airway health, we overexpressed elafin or secreted leukocyte protease inhibitor (SLPI, a molecule that also inhibits human neutrophil elastase (13)) in airway donors by adenovirus-mediated gene transfer (both of the vectors encode the secreted form of the proteinase inhibitor). The results showed that both elafin and SLPI overexpression were able to improve microvascular perfusion of the allografts 12 days following transplantation (Fig. 2H)

Systemic elafin administration prolongs airway microvascular perfusion and diminishes tissue hypoxia

Given the improvement in microvascular perfusion seen with the adenoviral elafin overexpression, we then tested systemic administration of recombinant human elafin. Consistent with the microvascular rejection kinetics observed with this strain combination in prior reports (6, 7), microvascular perfusion, as assessed by FITC-lectin perfusion, in saline treated control transplants was lost at d10, followed by a slow vascular regrowth from d12 to d18. However, in transplants treated with elafin, while there was still loss of perfusion at d10, there was improved microvascular perfusion starting on d12 and continuing through d18 (Fig. 3A and B). Consistent with the FITC-lectin perfusion, elafin treated allografts had higher airway tissue pO₂ and BPU from d12 to d18 following transplantation (Fig. 3C and D). We further showed that elafin treated allografts had better epithelial layer coverage and less subepithelial fibrotic remodeling (Fig. 3E)

Elafin diminishes the infiltration of neutrophils and macrophages but not T cells

Several lines of evidence have shown that elafin diminishes tissue inflammation through diverse mechanisms. Consistent with an earlier study (33), elafin treatment diminished neutrophil infiltration into acutely rejected airways as measured by myeloperoxidase (MPO) staining and is quantified as the mean fluorescent intensity (Fig. 4A and B). We further showed that on both d6 and 12, elafin therapy diminished neutrophil infiltration, and neutrophil infiltration into d12 allograft was less severe than that of d6 (Supplemental Fig. 1A and B). Because MPO is an enzyme associated with the production of ROS, we examined the levels of ROS by staining for DHE around the microvasculature endothelium. This showed that there was a reduction in the perivascular accumulation of ROS with elafin treatment (Fig. 4C and D). By using two markers commonly used to stain macrophages, F4/80 and MAC387, we found that elafin was also associated with diminished macrophage infiltration into grafts undergoing acute rejection (Supplemental Fig. 2A–D). We next demonstrated that elafin directly inhibited the chemotaxis of neutrophil in a concentration-dependent manner, whereas it had no effect on the migration of macrophages (Supplemental Fig. 3). T cells were also studied because they are known to play an essential role in airway rejection as previously described (24). Elafin treatment did not significantly affect the numbers of infiltrated CD4⁺ and CD8⁺ T cells in d8 allografts (Supplemental Fig. 4A–D). Together, these studies suggest that elafin treatment may diminish injurious tissue inflammation by attenuating the infiltration of innate immune cells; elafin may directly act on neutrophil and inhibit its migration.

Elafin diminishes microvascular complement deposition and endothelial cell apoptosis

As shown above (Fig. 3A), although elafin effectively promoted microvascular perfusion from d12 to d18, it was not able to completely protect the microvessels in d10 allografts. A similar phenomenon, characterized by a short-term perfusion loss during acute rejection, was observed in our previous study, in which we used mice in which the complement component, C3, was knocked out as transplant recipients (24). Interestingly, elastase has also been shown to cleave components of the complement system (34). We therefore hypothesized that elafin may attenuate complement activation. Indeed, the microvasculature of elafin treated d8 allografts had significantly lower levels of C3d deposition (Fig. 5A and D). Correspondingly, deposition of the membrane attack complex, C5b-9 (Fig. 5B and E) and endothelial cell apoptosis were also significantly diminished (Fig. 5C and F). These studies together suggest that elafin is able to protect endothelial cells from apoptosis likely by inhibiting injurious inflammation induced by neutrophils, macrophages and complement deposition.

Elafin promotes endothelial tube formation, migration and wound healing

Although elafin is better known as an inhibitor of neutrophil elastase, a very recent study revealed that this endogenous inhibitor can also directly promote tumor cell proliferation by activating the ERK mitogenic signaling pathway (35). We performed Western blot analysis of HUVECs and showed that elafin dose-dependently enhanced ERK1/2 activation (Fig. 6A). This implies that elafin may also directly promote endothelial proliferation and angiogenesis. To test this, we next carried out a series of angiogenesis assays, including the Matrigel tube formation assay, the migration assay and the scratch wound healing assay. Culture of HUVECs in Matrigel showed that elafin dose-dependently promoted tube formation (Fig. 6B–G, T and U). The migration (Fig. 6H–M, V) and scratch (Fig. 6N–S, W) assays showed that elafin promoted endothelial cell migration and wound healing capacity, respectively. At a concentration of 1.2 μ M, elafin was nearly as effective as VEGF in inducing endothelial cell tube formation, migration and wound healing (Fig. 6. T–W). These data demonstrate that elafin can act on endothelial cells to directly promote angiogenesis. A dose response assay further showed that 1.2 μ M elafin induces tube formation as potent as commonly used concentrations of VEGF in *in vitro* assays (0.6nM, 1.2nM) (Supplemental Fig. 5A and B), suggesting that high levels of elafin (μ M concentrations) may also potently promote angiogenesis *in vivo*.

CsA are known to induce EC injury and apoptosis (8), here we asked whether elafin is able to reverse the effect of CsA-induced EC injury. CsA, at a concentration of 0.1 μ M, slightly decreases EC tube formation (Fig. 7A), and elafin is able to promote tube formation at concentrations of both 0.6 and 1.2 μ M (Fig. 7A and B). However, 0.3 μ M CsA, a concentration that can be reached in transplant patients (36), significantly diminishes EC tube formation, and elafin is able to counter the injurious effect of CsA and promote the tube formation at a concentration of 1.2 μ M (Fig. 7A and B). These data suggested a protective role of elafin against CsA-induced EC damage.

Cyclosporine and elafin synergistically promote airway microvascular perfusion

Because CsA and elafin utilize distinct mechanisms to protect airway transplants, namely, by targeting adaptive immunity and innate immunity, respectively, we hypothesized that combination treatment with elafin and CsA may enhance the individual therapeutic efficacy of each drug. While neither elafin nor CsA alone was able to preserve microvascular perfusion, the combination of elafin and CsA (at a dose of 2.5mg/kg/d) synergistically promoted the perfusion of d10 allografts (Fig. 8A and B). Both BPU and airway tissue pO₂ studies showed a similar synergistic effect with elafin and CsA treatment (Fig. 8C and D). These data suggest that transplant microvascular health can be promoted by the simultaneous targeting of T cell and neutrophil-mediated immunity.

Discussion

Although neutrophils have long been known to be associated with transplant injury and the development of chronic rejection, no effective therapies have targeted neutrophils to prevent or reverse chronic rejection in solid organ transplantation. In the current study, we demonstrate that systemic administration of the neutrophil elastase inhibitor, elafin, was effective in protecting the microvascular circulation of airway transplants undergoing acute rejection and in expanding the incomplete therapeutic coverage of CsA. Consistent with our earlier findings (6), we again demonstrated that a healthier microvascular system preserves the airway epithelium and results in less fibrotic remodeling (Fig. 3E).

Following transplantation, the graft microvasculature encounters multiple insults including ischemia reperfusion injury and alloimmune attack (8, 32). Despite treatment with powerful immunosuppressants, the graft microvascular circulation sustains repetitive injury followed by inadequate regeneration which eventually leads to prolonged tissue hypoxia and accelerated fibrotic remodeling. Therefore, preservation of the graft microvasculature may represent a key strategy for preventing chronic rejection (8). Elafin may protect the microvasculature of transplant tissue through several mechanisms: 1) Elafin may reduce inflammation by preventing elastase-mediated elastin cleavage and accompanied tissue damage as shown in lung and colon models of bacterial infections (37–39). 2) Elafin also likely diminishes airway inflammation by attenuating the infiltration of neutrophils and macrophages. This is consistent with the described anti-inflammatory properties of elafin *in vitro* and *in vivo* (27, 37–39), and with previous findings that show that elastase may promote inflammation by activating receptors such as TLR4, and modulating the level of cytokines, such as IL-8 and monocyte chemoattractant protein (MCP-1) (40–42), which are potent chemo-attractants for neutrophils and monocytes/macrophages. Our data also suggested that elafin may attenuate neutrophil infiltration by directly inhibiting its migration. 3) Elafin can decrease complement activation and deposition on the endothelial cells of the microvasculature. Our data is consistent with earlier findings that showed that elastase is able to cleave and activate C3 (34), and that neutrophil elastase inhibition attenuates complement C5-mediated lung vascular injury (43). Moreover, since C5a promotes airway microvascular leakage and contributes to fibrotic remodeling of the allograft (25), elafin may also promote airway microvascular integrity by inhibiting C5 activation. Additionally, elafin may also promote angiogenesis by inhibiting the activation

of C3 as we suggested previously (24). 4) Elafin can decrease the production of perivascular ROS, whose production is catalyzed by neutrophil-produced myeloperoxidase. ROS is known to be one of the major mechanisms by which neutrophils can kill endothelial cells in transplants (44). 5) Lastly, elafin may directly act on endothelial cells as a mitogenic molecule and promote angiogenesis. Informed by a recent publication, in which elafin was demonstrated to promote cancer cell proliferation in an ERK activation-dependent manner (35), we also found that elafin is capable of activating ERK in endothelial cells and promoting endothelial cell proliferation, migration and tube formation in a dose-dependent manner (Fig. 6). At a concentration of 1.2 μ M, elafin is nearly as potent as VEGF in promoting angiogenesis. While it is not yet known how elafin activates the ERK pathway, this data suggests that the role of elafin as a potent proangiogenic molecule may be of significant importance in human physiology and pathophysiology. In addition, this mitogenic function of elafin may also protect ECs against CsA-induced injury (Fig. 7).

Cyclosporine is a calcineurin inhibitor that binds to cyclophilins and inhibits the transcription of IL-2 in T cells, which, in turn, prevents proliferation of activated T cells. The use of CsA has revolutionized the field of solid organ transplantation and the survival of transplant recipients has been dramatically improved since its introduction (e.g. (45)). However, a number of studies have shown that CsA is injurious to endothelial cells of kidney and heart transplants (46–48). While CsA did limit inflammation and partially protected the airway epithelium at doses of 2.5–25mg/kg/d, it was not able to maintain normal microvascular perfusion of the airway transplants. One possible explanation of this finding is that CsA is toxic to endothelial cells of the transplants undergoing acute rejection. However, the fact that CsA failed to preserve a normal airway microvascular circulation at all doses (2.5, 10 and 25mg/kg/d) tested, suggested that the suppression of T cell activity alone by CsA was not sufficient to overcome other factors that contribute to EC damage. ECs may be killed by other mechanisms such as the inflammation induced by cells of the innate immune system, including neutrophils and macrophages or through the complement system. Therefore, reducing neutrophil infiltration and associated inflammation is necessary and may be essential for enhancing transplant microvascular integrity and preventing the development of chronic rejection. However, we are also aware of the limitation of this relatively simplified tracheal transplant model we used, the complex microvascular system of a whole lung transplant may respond quite differently to the neutrophil and associated inflammation as well as therapeutic interventions.

In summary, this study indicates that the systemic administration of elafin fosters allograft microvascular perfusion and promotes the structural integrity of transplant tissue. Elafin may achieve its therapeutic effects by reducing inflammation, reducing the production of ROS and EC complement deposition, or by acting as an EC mitogen to directly promote angiogenesis. Our study suggests that the suppression of neutrophil elastase activity may represent a novel adjunctive therapy for transplant recipients suffering acute rejection.

Supplementary Material

Refer to Web version on PubMed Central for supplementary material.

Acknowledgments

This study was supported by NIH grants HL095686 and 1P01HL108797 and by a Veterans Affairs Merit Award BX000509 to M.R. Nicolls.

Abbreviations

ANOVA	analysis of variance
BAL	bronchoalveolar lavage
BPU	blood perfusion unit
C	complement
CsA	cyclosporine
DHE	Dihydroethidium
EC	endothelial cell
ECM	endothelial cell medium
ERK	extracellular signal-regulated kinase
HUVEC	human umbilical vein endothelial cell
IL	interleukin
LDF	laser doppler flowmetry
MFI	mean fluorescence intensity
MCP	monocyte chemotactic protein
MPO	myeloperoxidase
OB	obliterative bronchiolitis
PBS	phosphate-buffered saline
ROS	reactive oxygen species
SEM	standard error of the mean
SLPI	secreted leukocyte protease inhibitor
TLR	Toll-like receptor
TNF	tumor necrosis factor
TUNEL	terminal deoxynucleotidyl transferase-mediated dUTP nick end-labeling

References

1. Luckraz H, Goddard M, McNeil K, Atkinson C, Sharples LD, Wallwork J. Is obliterative bronchiolitis in lung transplantation associated with microvascular damage to small airways? *Ann Thorac Surg.* 2006; 82:1212–1218. [PubMed: 16996910]
2. Luckraz H, Goddard M, McNeil K, Atkinson C, Charman SC, Stewart S, Wallwork J. Microvascular changes in small airways predispose to obliterative bronchiolitis after lung transplantation. *J Heart Lung Transplant.* 2004; 23:527–531. [PubMed: 15135366]

3. Bishop GA, Waugh JA, Landers DV, Krensky AM, Hall BM. Microvascular destruction in renal transplant rejection. *Transplantation*. 1989; 48:408–414. [PubMed: 2476878]
4. Matsumoto Y, McCaughan GW, Painter DM, Bishop GA. Evidence that portal tract microvascular destruction precedes bile duct loss in human liver allograft rejection. *Transplantation*. 1993; 56:69–75. [PubMed: 8333070]
5. Revelo MP, Miller DV, Stehlik J, Brunisholz K, Drakos S, Gilbert EM, Everitt M, Budge D, Alharethi R, Snow G, et al. Longitudinal evaluation of microvessel density in survivors vs. nonsurvivors of cardiac pathologic antibody-mediated rejection. *Cardiovasc Pathol*. 2012; 21:445–454. [PubMed: 22381397]
6. Babu AN, Murakawa T, Thurman JM, Miller EJ, Henson PM, Zamora MR, Voelkel NF, Nicolls MR. Microvascular destruction identifies murine allografts that cannot be rescued from airway fibrosis. *J Clin Invest*. 2007; 117:3774–3785. [PubMed: 18060031]
7. Jiang X, Khan MA, Tian W, Beilke J, Natarajan R, Kosek J, Yoder MC, Semenza GL, Nicolls MR. Adenovirus-mediated HIF-1 α gene transfer promotes repair of mouse airway allograft microvasculature and attenuates chronic rejection. *J Clin Invest*. 2011; 121:2336–2349. [PubMed: 21606594]
8. Jiang X, Sung YK, Tian W, Qian J, Semenza GL, Nicolls MR. Graft microvascular disease in solid organ transplantation. *J Mol Med (Berl)*. 2014; 92:797–810. [PubMed: 24880953]
9. Aoki T, Tsuchida M, Takekubo M, Saito M, Sato K, Hayashi J. Neutrophil elastase inhibitor ameliorates reperfusion injury in a canine model of lung transplantation. *Eur Surg Res*. 2005; 37:274–280. [PubMed: 16374009]
10. Riise GC, Williams A, Kjellstrom C, Schersten H, Andersson BA, Kelly FJ. Bronchiolitis obliterans syndrome in lung transplant recipients is associated with increased neutrophil activity and decreased antioxidant status in the lung. *Eur Respir J*. 1998; 12:82–88. [PubMed: 9701419]
11. Zheng L, Walters EH, Ward C, Wang N, Orsida B, Whitford H, Williams TJ, Kotsimbos T, Snell GL. Airway neutrophilia in stable and bronchiolitis obliterans syndrome patients following lung transplantation. *Thorax*. 2000; 55:53–59. [PubMed: 10607802]
12. Todd JL, Wang X, Sugimoto S, Kennedy VE, Zhang HL, Pavlisko EN, Kelly FL, Huang H, Kreisel D, Palmer SM, et al. Hyaluronan contributes to bronchiolitis obliterans syndrome and stimulates lung allograft rejection through activation of innate immunity. *Am J Respir Crit Care Med*. 2014; 189:556–566. [PubMed: 24471427]
13. Henriksen PA. The potential of neutrophil elastase inhibitors as anti-inflammatory therapies. *Curr Opin Hematol*. 2014; 21:23–28. [PubMed: 24241342]
14. Smedly LA, Tonnesen MG, Sandhaus RA, Haslett C, Guthrie LA, Johnston RB Jr, Henson PM, Worthen GS. Neutrophil-mediated injury to endothelial cells. Enhancement by endotoxin and essential role of neutrophil elastase. *J Clin Invest*. 1986; 77:1233–1243. [PubMed: 3485659]
15. Furuno T, Mitsuyama T, Hidaka K, Tanaka T, Hara N. The role of neutrophil elastase in human pulmonary artery endothelial cell injury. *Int Arch Allergy Immunol*. 1997; 112:262–269. [PubMed: 9066513]
16. Nakatani K, Takeshita S, Tsujimoto H, Kawamura Y, Sekine I. Inhibitory effect of serine protease inhibitors on neutrophil-mediated endothelial cell injury. *J Leukoc Biol*. 2001; 69:241–247. [PubMed: 11272274]
17. Meyer KC, Nunley DR, Dauber JH, Iacono AT, Keenan RJ, Cornwell RD, Love RB. Neutrophils, unopposed neutrophil elastase, and alpha1-antiprotease defenses following human lung transplantation. *Am J Respir Crit Care Med*. 2001; 164:97–102. [PubMed: 11435246]
18. Moreau T, Baranger K, Dade S, Dallet-Choisy S, Guyot N, Zani ML. Multifaceted roles of human elafin and secretory leukocyte proteinase inhibitor (SLPI), two serine protease inhibitors of the chelonianin family. *Biochimie*. 2008; 90:284–295. [PubMed: 17964057]
19. Verrier T, Solhonne B, Sallenave JM, Garcia-Verdugo I. The WAP protein Trappin-2/Elafin: a handyman in the regulation of inflammatory and immune responses. *Int J Biochem Cell Biol*. 2012; 44:1377–1380. [PubMed: 22634606]
20. Sallenave JM. Secretory leukocyte protease inhibitor and elafin/trappin-2: versatile mucosal antimicrobials and regulators of immunity. *Am J Respir Cell Mol Biol*. 2010; 42:635–643. [PubMed: 20395631]

21. Cowan B, Baron O, Crack J, Coulber C, Wilson GJ, Rabinovitch M. Elafin, a serine elastase inhibitor, attenuates post-cardiac transplant coronary arteriopathy and reduces myocardial necrosis in rabbits after heterotopic cardiac transplantation. *J Clin Invest*. 1996; 97:2452–2468. [PubMed: 8647937]
22. Sato M, Keshavjee S, Liu M. Translational research: animal models of obliterative bronchiolitis after lung transplantation. *Am J Transplant*. 2009; 9:1981–1987. [PubMed: 19663891]
23. Jiang X, Hsu JL, Tian W, Yuan K, Olcholski M, de Perez VJ, Semenza GL, Nicolls MR. Tie2-dependent VHL knockdown promotes airway microvascular regeneration and attenuates invasive growth of *Aspergillus fumigatus*. *J Mol Med (Berl)*. 2013; 91:1081–1093. [PubMed: 23797537]
24. Khan MA, Jiang X, Dhillon G, Beilke J, Holers VM, Atkinson C, Tomlinson S, Nicolls MR. CD4+ T cells and complement independently mediate graft ischemia in the rejection of mouse orthotopic tracheal transplants. *Circ Res*. 2011; 109:1290–1301. [PubMed: 21998328]
25. Khan MA, Maasch C, Vater A, Klussmann S, Morser J, Leung LL, Atkinson C, Tomlinson S, Heeger PS, Nicolls MR. Targeting complement component 5a promotes vascular integrity and limits airway remodeling. *Proc Natl Acad Sci U S A*. 2013; 110:6061–6066. [PubMed: 23530212]
26. Sallenave JM, Xing Z, Simpson AJ, Graham FL, Gaudie J. Adenovirus-mediated expression of an elastase-specific inhibitor (elafin): a comparison of different promoters. *Gene Ther*. 1998; 5:352–360. [PubMed: 9614555]
27. Henriksen PA, Hitt M, Xing Z, Wang J, Haslett C, Riemersma RA, Webb DJ, Kotelevtsev YV, Sallenave JM. Adenoviral gene delivery of elafin and secretory leukocyte protease inhibitor attenuates NF-kappa B-dependent inflammatory responses of human endothelial cells and macrophages to atherogenic stimuli. *J Immunol*. 2004; 172:4535–4544. [PubMed: 15034071]
28. Jiang X, Malkovskiy AV, Tian W, Sung YK, Sun W, Hsu JL, Manickam S, Wagh D, Joubert LM, Semenza GL, et al. Promotion of airway anastomotic microvascular regeneration and alleviation of airway ischemia by deferoxamine nanoparticles. *Biomaterials*. 2014; 35:803–813. [PubMed: 24161166]
29. Kossodo S, Zhang J, Groves K, Cuneo GJ, Handy E, Morin J, Delaney J, Yared W, Rajopadhye M, Peterson JD. Noninvasive in vivo quantification of neutrophil elastase activity in acute experimental mouse lung injury. *Int J Mol Imaging*. 2011; 2011:581406. [PubMed: 21941648]
30. Khan MA, Dhillon G, Jiang X, Lin YC, Nicolls MR. New methods for monitoring dynamic airway tissue oxygenation and perfusion in experimental and clinical transplantation. *Am J Physiol Lung Cell Mol Physiol*. 2012; 303:L861–869. [PubMed: 23002078]
31. King MB, Jessurun J, Savik SK, Murray JJ, Hertz MI. Cyclosporine reduces development of obliterative bronchiolitis in a murine heterotopic airway model. *Transplantation*. 1997; 63:528–532. [PubMed: 9047145]
32. Jiang X, Tian W, Sung YK, Qian J, Nicolls MR. Macrophages in solid organ transplantation. *Vasc Cell*. 2014; 6:5. [PubMed: 24612731]
33. Hilgendorff A, Parai K, Ertsey R, Juliana Rey-Parra G, Thebaud B, Tamosiuniene R, Jain N, Navarro EF, Starcher BC, Nicolls MR, et al. Neonatal mice genetically modified to express the elastase inhibitor elafin are protected against the adverse effects of mechanical ventilation on lung growth. *Am J Physiol Lung Cell Mol Physiol*. 2012; 303:L215–227. [PubMed: 22683569]
34. Claesson R, Kanasi E, Johansson A, Kalfas S. A new cleavage site for elastase within the complement component 3. *APMIS*. 2010; 118:765–768. [PubMed: 20854470]
35. Labidi-Galy SI, Clauss A, Ng V, Duraisamy S, Elias KM, Piao HY, Bilal E, Davidowitz RA, Lu Y, Badalian-Very G, et al. Elafin drives poor outcome in high-grade serous ovarian cancers and basal-like breast tumors. *Oncogene*. 2014
36. Miller LW. Cyclosporine-associated neurotoxicity. The need for a better guide for immunosuppressive therapy. *Circulation*. 1996; 94:1209–1211. [PubMed: 8822970]
37. Simpson AJ, Wallace WA, Marsden ME, Govan JR, Porteous DJ, Haslett C, Sallenave JM. Adenoviral augmentation of elafin protects the lung against acute injury mediated by activated neutrophils and bacterial infection. *J Immunol*. 2001; 167:1778–1786. [PubMed: 11466403]
38. McMichael JW, Maxwell AI, Hayashi K, Taylor K, Wallace WA, Govan JR, Dorin JR, Sallenave JM. Antimicrobial activity of murine lung cells against *Staphylococcus aureus* is increased in vitro and in vivo after elafin gene transfer. *Infect Immun*. 2005; 73:3609–3617. [PubMed: 15908390]

39. Motta JP, Magne L, Descamps D, Rolland C, Squarzoni-Dale C, Rousset P, Martin L, Cenac N, Balloy V, Huerre M, et al. Modifying the protease, antiprotease pattern by elafin overexpression protects mice from colitis. *Gastroenterology*. 2011; 140:1272–1282. [PubMed: 21199654]
40. Pham CT. Neutrophil serine proteases: specific regulators of inflammation. *Nat Rev Immunol*. 2006; 6:541–550. [PubMed: 16799473]
41. Padrines M, Wolf M, Walz A, Baggiolini M. Interleukin-8 processing by neutrophil elastase, cathepsin G and proteinase-3. *FEBS Lett*. 1994; 352:231–235. [PubMed: 7925979]
42. Uehara A, Muramoto K, Takada H, Sugawara S. Neutrophil serine proteinases activate human nonepithelial cells to produce inflammatory cytokines through protease-activated receptor 2. *J Immunol*. 2003; 170:5690–5696. [PubMed: 12759451]
43. Hagio T, Nakao S, Matsuoka H, Matsumoto S, Kawabata K, Ohno H. Inhibition of neutrophil elastase activity attenuates complement-mediated lung injury in the hamster. *Eur J Pharmacol*. 2001; 426:131–138. [PubMed: 11525781]
44. Al-Lamki RS, Bradley JR, Pober JS. Endothelial cells in allograft rejection. *Transplantation*. 2008; 86:1340–1348. [PubMed: 19034000]
45. Parekh K, Trulock E, Patterson GA. Use of cyclosporine in lung transplantation. *Transplant Proc*. 2004; 36:318S–322S. [PubMed: 15041361]
46. Tepperman E, Ramzy D, Prodger J, Sheshgiri R, Badiwala M, Ross H, Raa V. Surgical biology for the clinician: vascular effects of immunosuppression. *Can J Surg*. 2010; 53:57–63. [PubMed: 20100415]
47. Trapp A, Weis M. The impact of immunosuppression on endothelial function. *J Cardiovasc Pharmacol*. 2005; 45:81–87. [PubMed: 15613984]
48. Petrakopoulou P, Anthopoulou L, Muscholl M, Klaus V, von Scheidt W, Uberfuhr P, Meiser BM, Reichart B, Weis M. Coronary endothelial vasomotor function and vascular remodeling in heart transplant recipients randomized for tacrolimus or cyclosporine immunosuppression. *J Am Coll Cardiol*. 2006; 47:1622–1629. [PubMed: 16631000]

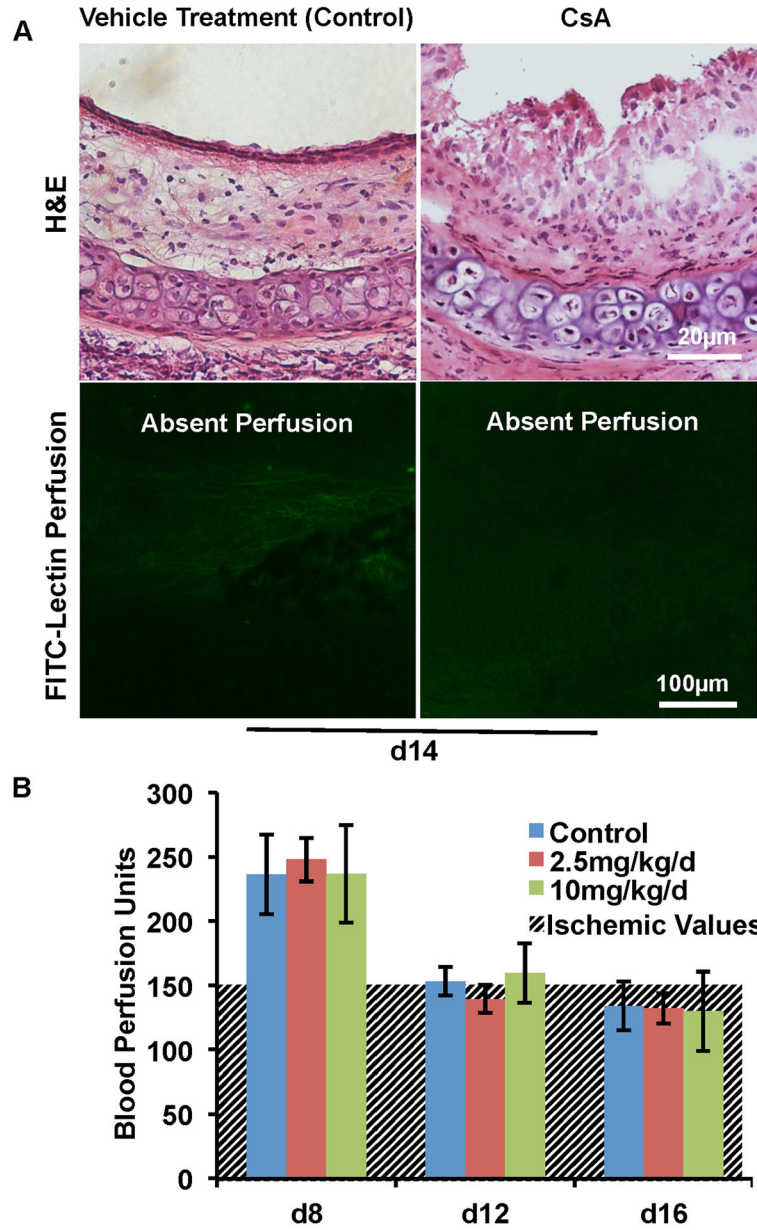


Figure 1. CsA does not protect the microvascular circulation of airway transplants (A) H&E staining (top row) and FITC-lectin perfusion (bottom row) of d14 allografts. CsA was administered at a dose of 25mg/kg/d. CsA partially protected the epithelial layer (top row), but did not preserve microvascular perfusion (bottom row). (B) BPU studies showed that CsA administered at doses of both 2.5 and 10mg/kg/d did not improve airway blood perfusion compared with controls (n=4–6 per group). The hatched line background represents values at which ischemia is demonstrated by FITC-lectin staining. BPUs are arbitrary values determined by the doppler flowmetry device. Scale bars, 20µm (A, top row) and 100µm (A, bottom row). Data are shown as mean±SEM.

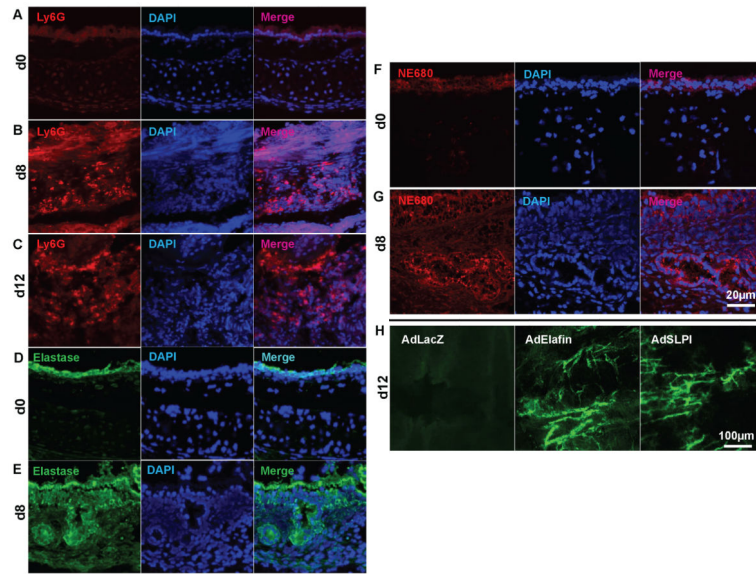


Figure 2. Increased neutrophil infiltration into airway transplants undergoing acute rejection (A–C) Neutrophil infiltration, identified by Ly6G staining, into normal tracheas (A), d8 transplants (B) and d12 transplants (C). (D–E) Expression of elastase in normal tracheas (D) and d8 transplants (E). (F–G) Elastase activity in normal tracheas (F) and d8 transplants (G). (H) FITC-lectin perfusion imaging showing that adenovirus-mediated elafin or SPLI transduction protected the microvascular circulation of d12 airway transplants (n=4–6, representative image shown). Scale bars, 20µm (A–G) and 100µm (H).

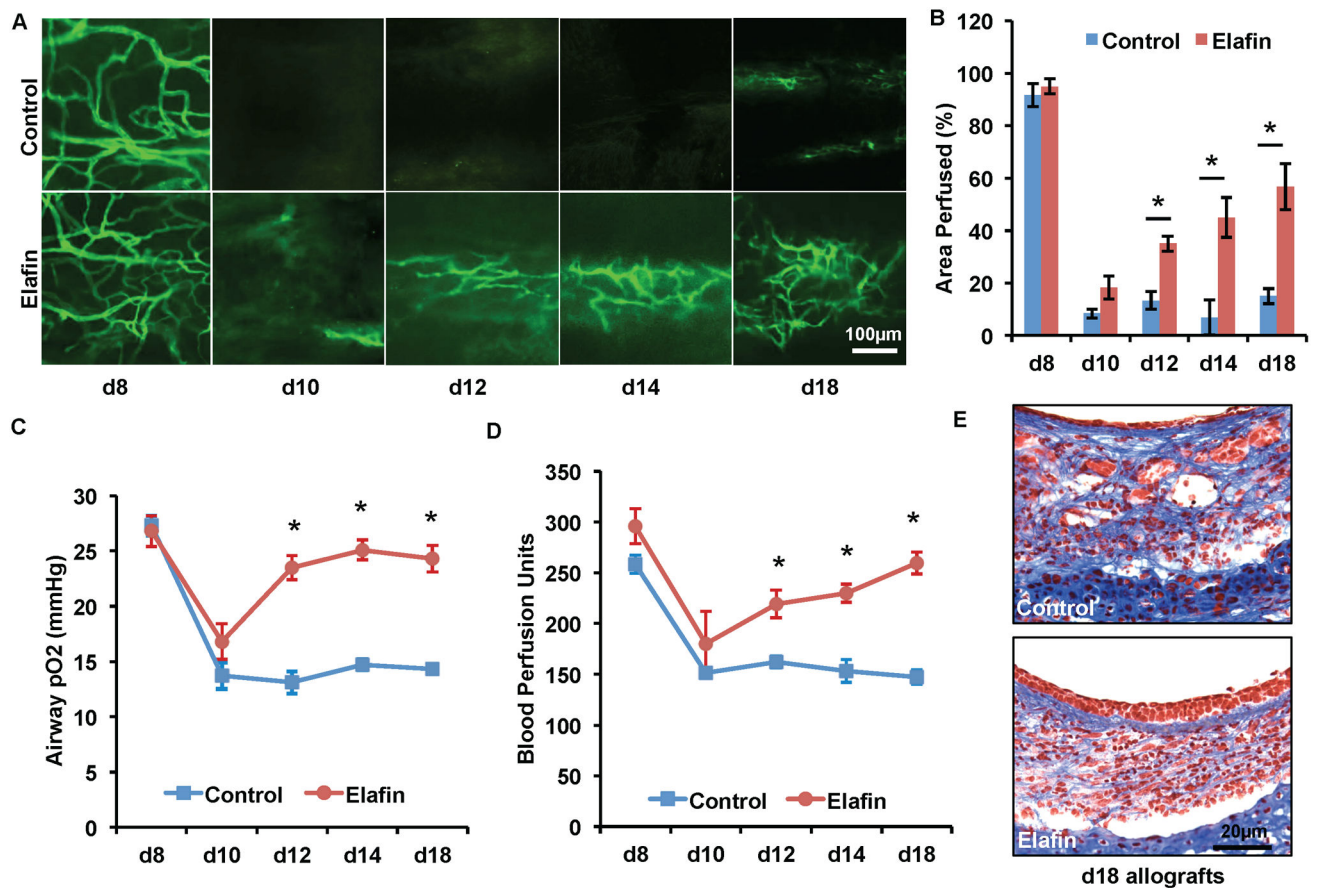


Figure 3. Systemic elafin administration prolongs airway microvascular perfusion, diminishes airway hypoxia and attenuates airway fibrotic remodeling

(A) FITC-lectin perfusion imaging showing that elafin (1.9mg/kg/d starting on d0) treatment prolongs airway microvascular perfusion. (B) Quantification of perfused areas of the trachea transplant. (C) Airway tissue pO₂ measurement following transplantation. (D) Blood perfusion units measured by laser doppler flowmetry. (E) Masson's Trichrome staining showed that elafin-treated tracheas at d18 display more normal epithelial layer and less subepithelial fibrosis (n=4–6, representative image shown). Scale bars, 100µm (A) and 20µm (E). Data are shown as mean±SEM. Individual time points were compared with the Student's t test. *P<0.05.

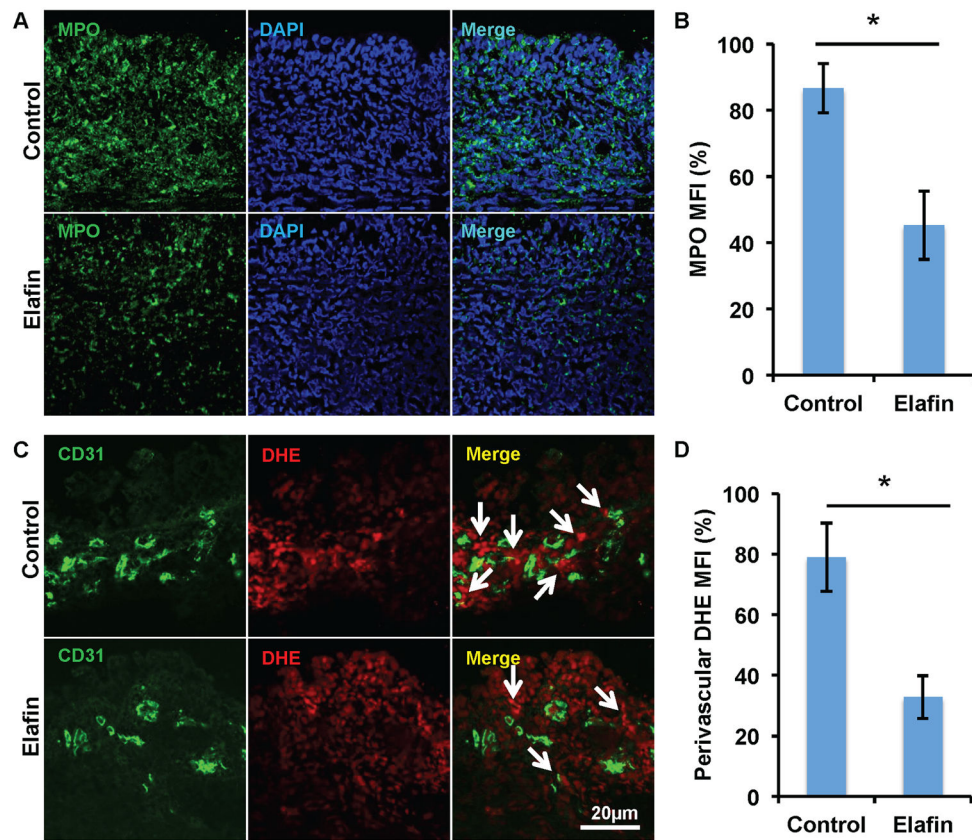


Figure 4. Elafin administration diminishes neutrophil infiltration and the production of perivascular ROS

(A) Myeloperoxidase (MPO) staining showing decreased neutrophil infiltration into d8 transplants following elafin treatment. (B) Quantification of mean fluorescence intensity (MFI) of MPO staining (n=3–5 per group). (C) Detection of ROS by DHE staining showing decreased perivascular ROS production (white arrows) in elafin-treated allografts. (D) Quantification of perivascular MFI of DHE staining (n=3–5 per group). Scale bars, 20 μ m (A and C). Data are shown as mean \pm SEM. Student's t test was used to compare groups. *P<0.05.

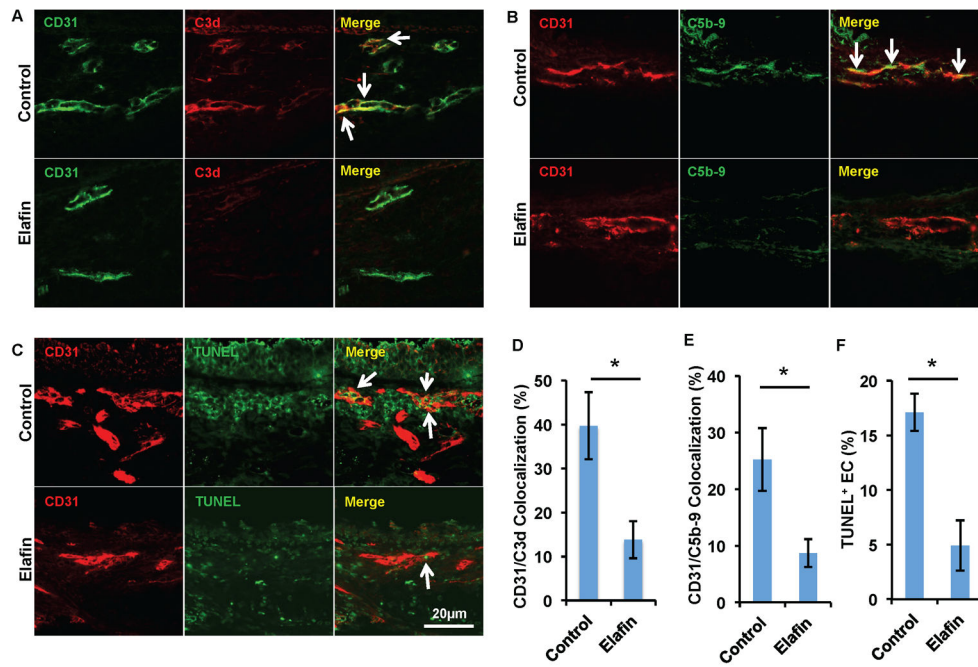


Figure 5. Elafin diminishes complement deposition on airway microvasculature
 (A) Immunofluorescence imaging shows less C3d deposition on ECs (white arrows) in allografts treated with elafin. (B) ECs of allografts treated with elafin have less deposition of C5b-9 complex. (C) EC TUNEL staining shows decreased EC apoptosis in allografts treated with elafin. (D–F) Quantification of C3d deposition (D), C5b-9 deposition (E) and EC TUNEL staining (F) (n=6 per group, representative image shown). Scale bars, 20µm (A–C). Data are shown as mean±SEM. Student’s t test was used to compare groups. *P<0.05.

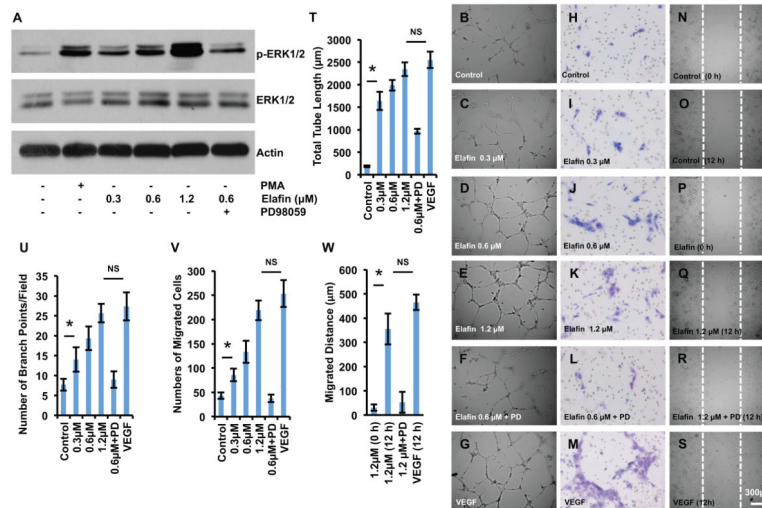


Figure 6. Elafin promotes HUVEC tube formation, migration and wound healing (A) Western Blot analysis showing that elafin dose-dependently induces ERK1/2 phosphorylation. PMA was used as a positive control for ERK1/2 phosphorylation, the ERK1/2 inhibitor, PD098059, was used at a concentration of 10μM. (B–S) Elafin dose-dependently promotes HUVEC tube formation (B–G) as measured by the Matrigel assay, HUVEC migration as measured by the Boyden Chamber assay (H–M), and HUVEC wound healing assay (N–S). VEGF was used as a positive control. (T–W) Quantification of total tube length (T), number of branch points per field (U), number of migrated cells in Boyden Chamber assay (V) and number of migrated cells in wound healing assay (W). (n=4–6 per group). Scale bar, 300μm (B–S). Data are shown as mean±SEM. Student’s t test (T–V) or 1-way ANOVA with Tukey’s post test (W). *P<0.05; NS, not significant.

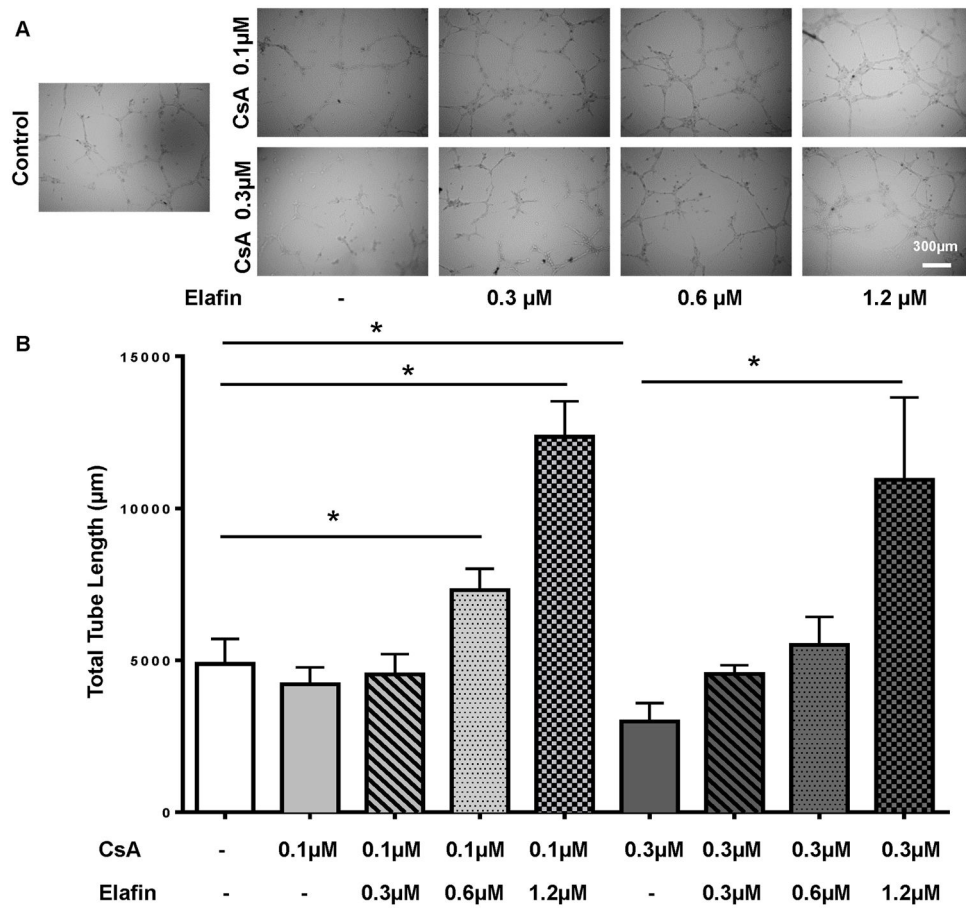


Figure 7. Elafin promotes tube formation in the presence of CsA

(A) Tube formation assay with different concentrations of CsA (0.1 µM and 0.3 µM) and elafin (0.3 µM, 0.6 µM and 1.2 µM). (B) Quantification of the tube formation assay. Scale bar, 300µm (A). Data are shown as mean±SEM. One-way ANOVA with Tukey’s post test (B). *P<0.05.

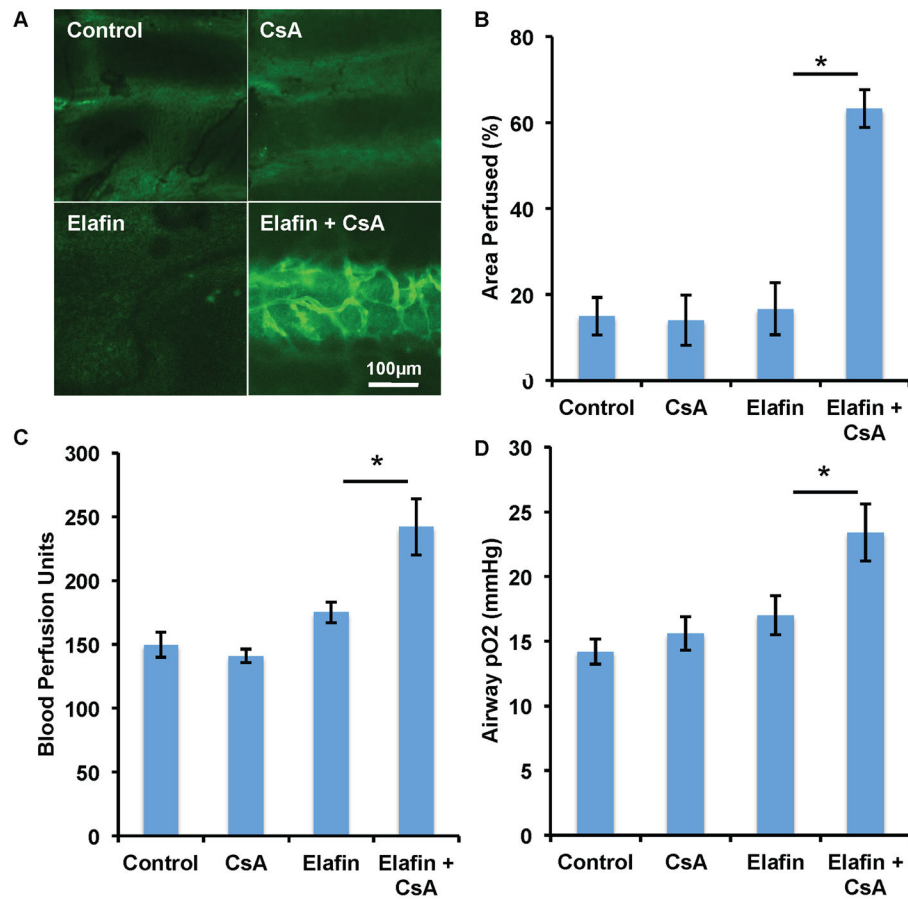


Figure 8. Cyclosporine and elafin synergistically promote airway microvascular perfusion and oxygenation

(A) FITC-lectin perfusion image showing that neither elafin (1.9mg/kg/d) nor CsA (2.5mg/kg/d) is able to preserve microvascular circulation of d10 allografts, but the combination of elafin and CsA therapy protects the microvascular circulation. (B) Quantification of perfused area. (C, D) Both blood perfusion unit study (C) and tissue pO₂ examination (D) showed the synergistic effect of elafin and CsA (n=4–6 per group). Scale bar, 100 μ m (A). Data are shown as mean \pm SEM. Student's t test was used to compare groups. *P<0.05.